# Photodissociation of van der Waals clusters of isoprene with oxygen, $C_5H_8$-$O_2$, in the wavelength range 213–277 nm

Konstantin V. Vidma, Pim W. J. M. Frederix, David H. Parker, and Alexey V. Baklanov

Citation: The Journal of Chemical Physics **137**, 054305 (2012); doi: 10.1063/1.4737856
View online: http://dx.doi.org/10.1063/1.4737856
View Table of Contents: http://aip.scitation.org/toc/jcp/137/5
Published by the American Institute of Physics

# Photodissociation of van der Waals clusters of isoprene with oxygen, $C_5H_8-O_2$, in the wavelength range 213–277 nm

Konstantin V. Vidma,[1] Pim W. J. M. Frederix,[1] David H. Parker,[1] and Alexey V. Baklanov[2]
[1]*Institute for Molecules and Materials, Radboud University Nijmegen, Heyendaalseweg 135, 6525 ED Nijmegen, The Netherlands*
[2]*Institute of Chemical Kinetics and Combustion, Institutskaja Street 3, Novosibirsk 630090 Russia and Novosibirsk State University, Pirogova street 2, Novosibirsk 630090, Russia*

(Received 7 March 2012; accepted 5 July 2012; published online 2 August 2012)

The speed and angular distribution of O atoms arising from the photofragmentation of $C_5H_8-O_2$, the isoprene-oxygen van der Waals complex, in the wavelength region of 213–277 nm has been studied with the use of a two-color dissociation-probe method and the velocity map imaging technique. Dramatic enhancement in the O atoms photo-generation cross section in comparison with the photodissociation of individual $O_2$ molecules has been observed. Velocity map images of these "enhanced" O atoms consisted of five channels, different in their kinetic energy, angular distribution, and wavelength dependence. Three channels are deduced to be due to the one-quantum excitation of the $C_5H_8-O_2$ complex into the perturbed Herzberg III state ($^3\Delta_u$) of $O_2$. This excitation results in the prompt dissociation of the complex giving rise to products $C_5H_8+O+O$ when the energy of exciting quantum is higher than the complex photodissociation threshold, which is found to be 41740 $\pm$ 200 $cm^{-1}$ (239.6$\pm$1.2 nm). This last threshold corresponds to the photodissociation giving rise to an unexcited isoprene molecule. The second channel, with threshold shifted to the blue by 1480 $\pm$ 280 $cm^{-1}$, corresponds to dissociation with formation of rovibrationally excited isoprene. A third channel was observed at wavelengths up to 243 nm with excitation below the upper photodissociation threshold. This channel is attributed to dissociation with the formation of a bound O atom $C_5H_8-O_2 + h\nu \rightarrow C_5H_8-O_2(^3\Delta_u) \rightarrow C_5H_8O + O$ and/or to dissociation of $O_2$ with borrowing of the lacking energy from incompletely cooled complex internal degrees of freedom $C_5H_8{}^*-O_2 + h\nu \rightarrow C_5H_8{}^*-O_2(^3\Delta_u) \rightarrow C_5H_8 + O + O$. The kinetic energy of the O atoms arising in two other observed channels corresponds to O atoms produced by photodissociation of molecular oxygen in the excited $a\,^1\Delta_g$ and $b\,^1\Sigma_g^+$ singlet states as the precursors. This indicates the formation of singlet oxygen $O_2(a\,^1\Delta_g)$ and $O_2(b\,^1\Sigma_g^+)$ after excitation of the $C_5H_8-O_2$ complex. Cooperative excitation of the complex with a simultaneous change of the spin of both partners $^1X-{}^3O_2 + h\nu \rightarrow {}^3X-{}^1O_2 \rightarrow {}^3X + {}^1O_2$ is suggested as a source of singlet oxygen $O_2(a\,^1\Delta_g)$ and $O_2(b\,^1\Sigma_g^+)$. This cooperative excitation is in agreement with little or no vibrational excitation of $O_2(a\,^1\Delta_g)$, produced from the $C_5H_8-O_2$ complex as studied in the current paper as well as from the $C_3H_6-O_2$ and $CH_3I-O_2$ complexes reported in our previous paper [Baklanov *et al.*, J. Chem. Phys. **126**, 124316 (2007)]. The formation of $O_2(a\,^1\Delta_g)$ from $C_5H_8-O_2$ was observed at $\lambda_{pump}$ = 213–277 nm with the yield going down towards the long wavelength edge of this interval. This spectral profile is interpreted as the red-side wing of the band of a cooperative transition $^1X-{}^3O_2 + h\nu \rightarrow {}^3X(T_2)-{}^1O_2(a\,^1\Delta_g)$ in the $C_5H_8-O_2$ complex. © *2012 American Institute of Physics*. [http://dx.doi.org/10.1063/1.4737856]

## I. INTRODUCTION

Photoabsorption and photodissociation of molecular oxygen by radiation in the ultraviolet (UV) region strongly depends on the molecular environment of $O_2$.[1] Individual $O_2$ molecules are essentially transparent in the IR, visible, and UV regions[2] due to the fact that all optical transitions corresponding to this range are forbidden by spin or orbital symmetry selection rules. In the UV range, the most important for photochemistry, molecular oxygen has two weak absorption bands: the discrete Herzberg bands (300–242 nm) and the Herzberg continuum (200–242 nm). Both of these features correspond to transitions to the bound or repulsive parts of three states called Herzberg I ($A\,^3\Sigma_u^+$), Herzberg II ($c\,^1\Sigma_u^-$), and Herzberg III ($A'\,^3\Delta_u$).[2]

In the presence of a molecular environment the spectroscopic behavior of $O_2$ changes dramatically. In numerous previous spectroscopic studies strong enhancement of the UV absorption of $O_2$ is reported. A review of the literature related to this topic is given in our previous paper.[1] Enhancement in UV absorption of $O_2$ is observed in the liquid, solid, and gas phase, and the main contribution to the enhancement is provided by the Herzberg III state.[3–12]

One-to-one van der Waals complexes of oxygen, $X-O_2$, are very convenient model systems for investigation of the mechanisms of primary photochemical processes taking place when $O_2$ molecules are in the presence of neighboring molecules in the liquid and solid phase, or during collisions in gas phase. The UV-photodissociation of these complexes, which are generated in pulsed molecular

 

beams, has been studied with the use of the time-of-flight mass-spectrometry[13–15] and with velocity map imaging of the photofragment O atom.[1,16] In our previous paper[1] we studied the photodissociation of $X-O_2$ clusters ($X=CH_3I$, $C_3H_6$ (propylene), $C_6H_{12}$, Xe) at the dissociation wavelength 226 nm with detection of $O(^3P_2)$ products by means of the velocity map imaging technique in its slicing modification.[17] In that study we gave a critical review of previous work on $X-O_2$ clusters and reported results of experiments which reveal a dramatic difference in the photophysics and photochemistry of oxygen in complexes as compared with the "free" $O_2$ molecule. This difference involves not only enhancement of the $O_2$ UV-photoabsorption cross section in the complex by the orders of magnitude as compared with the "free" $O_2$ molecule, as observed earlier,[13–16] but also the appearance of the new photochemistry. Five channels (labeled in[1] as C1–C5) of enhanced formation of O atoms differing in their kinetic energy and angular anisotropy of recoil directions were observed.[1] Based on the obtained results we concluded that for those clusters two mechanisms of absorption enhancement take place. First, a contribution is provided by enhancement of the transition to the Herzberg state of $O_2$ (mainly to the Herzberg III state), perturbed by the admixture of the charge-transfer (CT) state of the complex. The second contribution was suggested to be due to the direct transition into ($X^+-O_2^-$), the charge-transfer state of the complex. Possible dissociation pathways leading to the formation of each of the observed channels of $O(^3P_2)$ atoms were proposed. The main channel, labeled C1, was assigned to be a result of the excitation into a perturbed covalent state. The observed negative anisotropy of C1 was shown to be a result of the admixing of the charge-transfer nature of the transition and of the T-shaped geometry of the complex. Analysis of the energy and anisotropy of that channel allowed us to extract information about the dynamics of the photodissociation and to determine the values of the van der Waals binding energy in the $CH_3I-O_2$, $Xe-O_2$, $C_6H_{12}-O_2$, and $C_3H_6-O_2$ clusters.[18]

In the present study, we have performed experiments on the photodissociation of $C_5H_8-O_2$, the isoprene-oxygen complex. Investigation of these clusters is interesting from the point of view of atmospheric photochemistry, because isoprene is the second most abundant biogenic volatile organic compound in the earth's atmosphere.[19] We have modified the experimental approach as compared with paper[1] where the same laser pulse was used to excite the complex and probe the O atom photofragment in one-laser experiments. In the current paper, we have used a two-laser dissociation-probe experimental setup that allows us to broaden the range of the photoexcitation wavelengths to 213–277 nm. The main interest was focused on the evolution of the properties of the observed channels with variation of the excitation wavelengths as well as on testifying the earlier suggested models of the UV-photophysics and photochemistry of $X-O_2$ van der Waals complexes.

## II. EXPERIMENT

The experiments were performed in a differentially pumped vacuum chamber equipped with a velocity map imaging assembly[20] and a pulsed valve (Jordan) mounted in the on-axis configuration. The valve created the supersonic molecular beam by opening a 0.5 mm nozzle for about 100 $\mu$s. In order to create the $C_5H_8-O_2$ clusters the valve was filled with a gas mixture of $C_5H_8$(0.5%) + $O_2$(5%) + He(94.5%). The total backing pressure of the gas in the valve in all experiments (unless explicitly mentioned) was 1 bar. After supersonic expansion into the vacuum chamber, the beam was skimmed by a 2 mm skimmer mounted 15 mm downstream from the nozzle, and introduced into the photoexcitation region by passing through the 2 mm diameter hole in the repeller electrode, mounted about 55 mm downstream from the nozzle. The design of electrodes of the velocity map imaging assembly was similar to the setup described in Ref. 21. In the photoexcitation region the molecular beam was irradiated by a sequence of two pulses of UV radiation, counter-propagating at a right angle with the molecular beam propagation direction.

The first pulse of UV radiation (the "pump laser") was used for the photodissociation of $C_5H_8-O_2$. The wavelength of the pump laser was tuned in the range of 222–277 nm or was fixed at 213 nm. All wavelengths given in this paper are vacuum wavelengths. Radiation in the range of 222–277 nm was obtained by frequency doubling (using a beta barium borate (BBO) crystal), the output of a optical parametric oscillator (Spectra-Physics Quanta-Ray MOPO-HF system), pumped by the third harmonic of a Nd:YAG laser (Quanta Ray PRO-Series). Pump radiation with the wavelength of 213 nm was obtained by generation of the fifth harmonic of a Nd:YAG laser (Quanta Ray, GCR-11).

At all wavelengths used, the resulting energy of the pump laser was ~3–4 mJ and the pulse duration was about 5 ns. The laser beam with a diameter of about 8 mm was focused with a f = 22 cm lens. The focal point was shifted ~5 mm from the center of the molecular beam.

The second pulse of UV radiation (the "probe laser") was used for selective ionization of $O(^3P_J)$ atoms arising in the photodissociation of the clusters. This pulse was obtained by frequency doubling (in a BBO crystal) the output of pulsed dye laser (Quanta Ray, PDL-2, Coumarin 47), pumped by the third harmonic of Nd:YAG laser (Continuum Surelite III–10). In major part of experiments the wavelength of the probe laser was fixed at 226.234 nm in order to provide resonance enhanced multiphoton ionization (REMPI) of $O(^3P_0)$ atoms via the intermediate $(2s^2 2p^3(^4S_0)3p)$ state.[22] The energy of the resulting probe radiation was around 1 mJ and the pulse duration was about 5 ns. The beam size was ~3 mm. The pump radiation was focused with a f = 20 cm lens. The focal point was also shifted around 5 mm behind the molecular beam.

The time delay between the pump and probe laser pulse was around 100 ns. The polarization direction of the linearly polarized pump and probe laser beams was controlled using variable retardation plates (Alphalas). The directions of the polarization of the pump and probe laser were parallel to each other and perpendicular to the molecular beam propagation direction. The wavelengths of both pump and probe lasers were calibrated and measured by a wavelength meter (High Finesse, WS-7).

Ions produced by the two pulses were extracted from the photoexcitation region, accelerated and projected on the surface of the MCP + phosphor screen detector. In order to provide the detection of $O^+$ ions, the detector was gated at a time corresponding to the time of flight of ions with a mass of 16 amu.

The obtained raw images were inverted using the BASEX inversion algorithm.[23] For every pump wavelength the image of $O(^3P_0)$ originated from the photodissociation of pure $O_2$ was recorded for kinetic energy calibration of images. The rings corresponding to one photon dissociation to the first dissociation limit ($O(^3P) + O(^3P)$) and two-photon dissociation to the second dissociation limit ($O(^3P) + O(^1D)$) were used for calibration. In the calibration experiments the valve was filled with pure $O_2$ at a pressure of 1 bar.

The valve, detector, and all lasers except the MOPO-HF were operating with a repetition rate of 10 Hz. The MOPO-HF laser was working at a repetition rate of 20 Hz, and only every second pulse was used in the experiments.

## III. RESULTS

Raw images of $O^+$ ions arising in the two-color experiments at several wavelengths of the pump laser in the range of 213–242 nm are shown in Fig. 1, and in Fig. 2 the speed distribution extracted from the analysis of those images is presented. All observed $O^+$ signal corresponds to the resonant ionization of $O(^3P_0)$ atoms by the probe laser; slight detuning of the wavelength from the resonance leads to the complete disappearance of signal. We discuss the reasons for presenting only $O(^3P_0)$ images at the end of this section after describing the observed signal. Basically, the same information is obtained from $O(^3P_2)$ and $O(^3P_1)$ images, only with different relative yields. From the $O(^3P_0)$ images shown here we distinguished five channels that differ by kinetic energy, angular distribution, and by their wavelength dependence. The different channels are shown by arrows on Figs. 1 and 2. The enumeration of the channels C1, C2, C4, and C5 is copied from Ref. 1 since we believe that these channels are produced in the mechanism similar to the channels observed in that study.

In all experiments with clusters the absolute value of the $O(^3P_0)$ signal was much stronger than in experiments with individual molecules at similar laser power, even though the concentration of $O_2$ in the experiments on pure $O_2$ was at least 20 times higher than that in cluster experiments. In the images obtained for cluster conditions no contributions from unclustered molecules of $O_2$ were detected.

Two-color images presented in Fig. 1 were obtained by subtraction of the one-laser signal given by the probe laser only from the total signal. This subtraction was not always straightforward due to substantial depletion of ground state clusters $C_5H_8-O_2$ caused by the pump laser. Therefore, for subtraction, the one-color image originating from the probe laser was multiplied by a factor smaller than one. The value of this factor was adjusted manually in order to provide full disappearance of the features specific for one-color signal and at the same time keep the signal from becoming negative. A typical value of this coefficient was around 0.4, which reflects

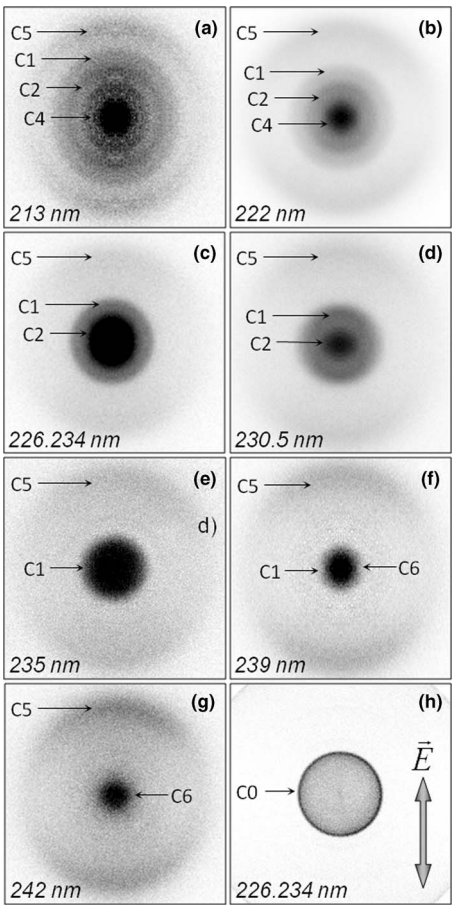


FIG. 1. (a)–(g) Images of $O(^3P0)$ atoms resulting from the excitation of $C_5H_8-O_2$ clusters in the wavelength region of 213–242 nm. Images (a–b) and (d–g) correspond to two-color experiments, with the wavelength of the pump laser shown in each image. For these images the one-laser signal resulting from the probe laser only was subtracted from the raw images. Image (c) was obtained in a one-laser experiment, where the excitation and (2+1) REMPI of $O(^3P_0)$ atoms were both provided by 226.234 nm light. Image (h) is from $O(^3P_0)$ atoms resulting from the one-color experiments on unclustered O2 at the wavelength of 226.234 nm. Separate rings in the images are labeled by channel numbers C0–C6 as given in Ref. 1. C3 from Ref. 1 is not observed in this study. The ring C0 shown in image (h) corresponds to an average kinetic energy of one O atom of 1314.2 $cm^{-1}$ (0.163 eV) or 1402 m/s. The double-headed arrow in (h) indicates the direction of the linear polarization of both the pump and probe lasers. Image size is scaled to C5, the relative size of the other rings varies thus with photolysis laser wavelength.

the fraction of clusters $C_5H_8-O_2$ remaining unexcited after the first laser pulse.

Channels C1 and C2 appeared as relatively sharp rings with their size depending on the pump laser wavelength. The dependence of the $O(^3P_0)$ atom kinetic energy of channels C1 and C2 on the pump laser photon energy is presented in Fig. 3. Note that the photon energy is plotted on the vertical axis and $O(^3P_0)$ atom kinetic energy is plotted on the horizontal axis. Both dependencies can be well approximated by linear fits (Figs. 3(a) and 3(b)). From the fit, the appearance thresholds for those channels were found to be $41740 \pm 200$ $cm^{-1}$ ($239.6 \pm 1.2$ nm) and $43220 \pm 190$ $cm^{-1}$ ($231.4 \pm 1.0$ nm) for channels C1 and C2, respectively. When the pump laser photon energy was lower than the threshold of appearance of channel C1, some signal around the center of the image was still observed (Fig. 1(g)). It was observed at

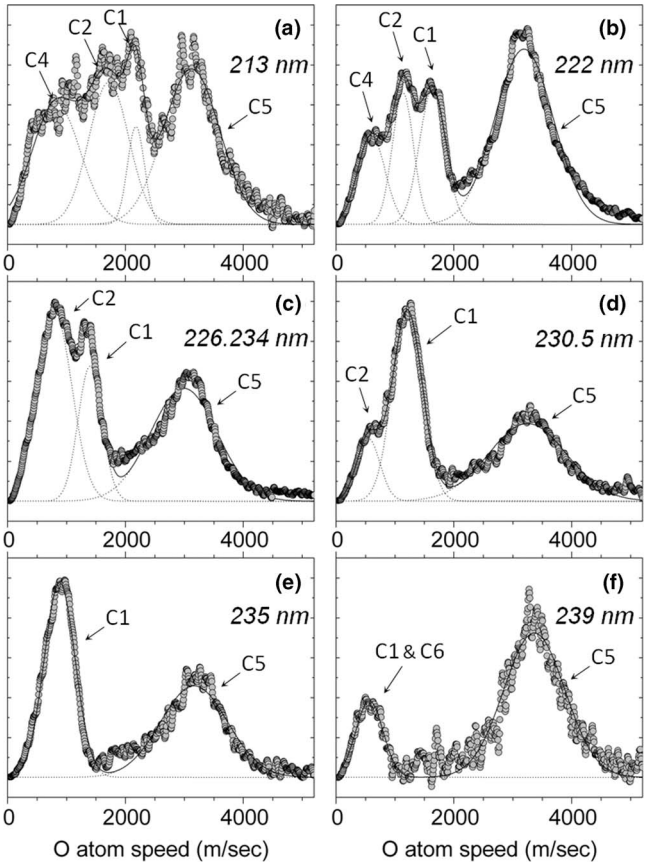


FIG. 2. Speed distribution of $O(^3P_0)$ atoms taken from the analysis of the inverted images shown. Figures (a–b), (d–f) correspond to two-color images with the wavelength of the first laser shown in each figure. Figure (c) corresponds to the one laser experiment when the 226.234 nm laser pulse was used for both excitation and REMPI of $O(^3P_0)$ atoms. Experimental points are shown by open circles. The experimental distributions were fit by a sum of Gaussian curves with the use of one Gaussian for each channel. The result of the fit is shown by the solid line, and each individual Gaussian is shown by a dotted line. In graph (f), channels C1 and C6 are indistinguishable; they both might contribute to the Gaussian curve centered on 500 m/sec.

least until 243 nm and disappeared between 243 and 245 nm. We attribute this signal to a new channel, C6.

Channel C4 appears as a blob in the middle of the image that first appeared between 222 nm and 226.234 nm and was observed as a blob of larger size at $\lambda_{pump} = 213$ nm.

Channel C5 appears as a relatively broad ring with a large size. The radius of the ring was found to be only slightly dependent on the pump laser wavelength and corresponded to the kinetic energy of O atoms in the range of 0.74 $\pm$ 0.05 eV. The signal corresponding to this channel started to appear between 277 and 260 nm and was observed at all shorter wavelengths down to 213 nm.

For each of the observed channels the dependence of the intensity of the signal on the angle $\theta$ between the laser polarization and the direction of recoil of the O atom has been extracted and fitted with the following expression:

$$\frac{dN}{d\Omega} \propto \left(1 + \beta \cdot \left(\frac{3}{2}\cos^2\theta - \frac{1}{2}\right)\right). \quad (1)$$

Equation (1) represents the general case of the angular distribution of fragments produced in a one-photon dissociation

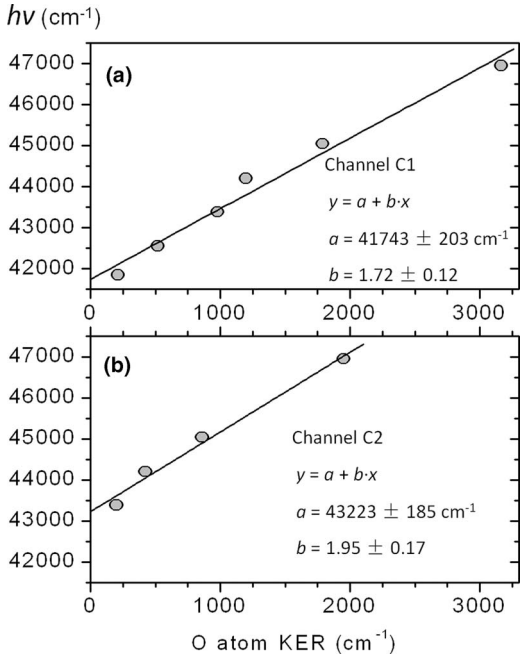


FIG. 3. Linear fits of the dependency of the kinetic energy of O atoms corresponding to channels C1 and C2 on the excitation photon energy. (a) Channel C1; (b) Channel C2. Vertical axis: photon energy, horizontal axis: kinetic energy of the O atom.

process.[24] In this equation $\beta$ is the so-called anisotropy parameter that can have a value between $-1$ to 2. For channels C1 and C2 the values of $\beta$ were determined from the fitting and were plotted as a function of the excitation wavelength in Fig. 4. For these channels a systematic reduction of the measured $\beta$ values was observed with shifting of excitation wavelength to the red. For the channels C4 and C6, which appear as blobs, the anisotropy was not well pronounced and a reliable extraction of $\beta$ was impossible.

In order to check the size of the cluster giving rise to the observed signals, we measured the dependence of the intensity of different parts of the image on the total backing

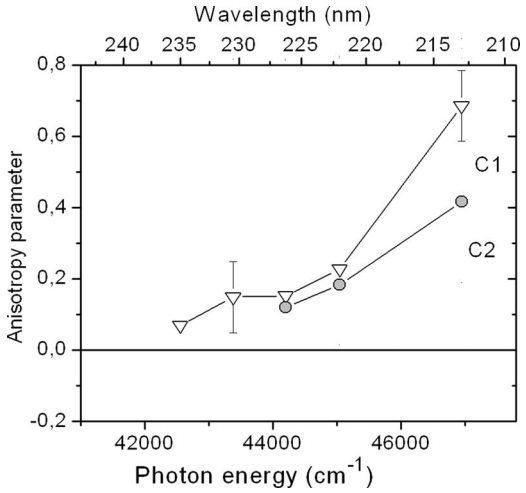


FIG. 4. The measured value of the anisotropy parameter $\beta$ for channels C1 and C2 of formation of $O(^3P_0)$, as a function of the pump laser wavelength. The scatter of the measured values for channel C1 are shown by the error bars. The scatter for channel C2 is similar to that for C1.

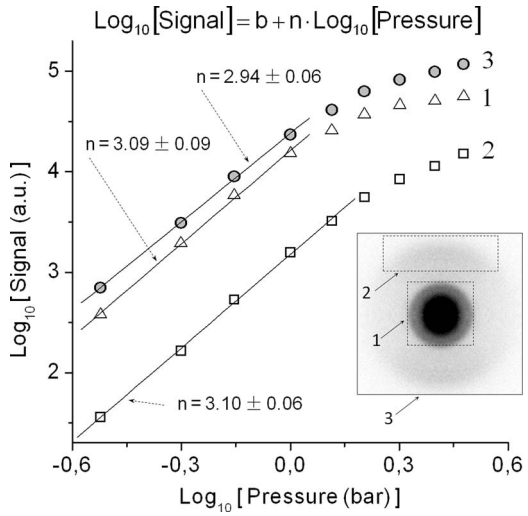


FIG. 5. Backing pressure dependence of the integral signal from different parts of the image of $O(^3P_0)$ atoms arising in the one-color dissociation of $C_5H_8-O_2$ clusters at the wavelength of 226.234 nm. The dependence is shown in a log-log scale. Symbols correspond to the experimental points and solid lines are their least squared linear fittings with formula: $Log_{10}$ [Signal] = b + n.$Log_{10}$ [Pressure]. Data is labeled as follows: 1–signal from central part, 2–signal from external part, 3–the total signal of the image shown in the inset.

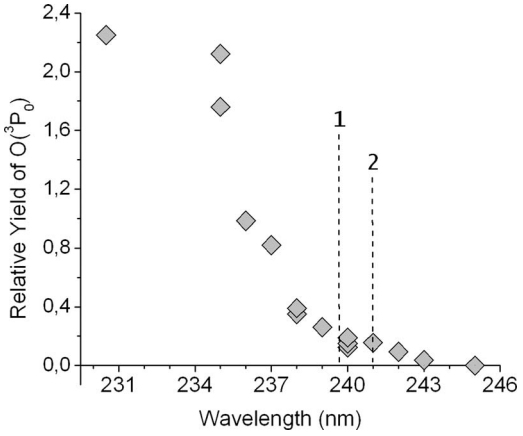


FIG. 6. Relative yield of $O(^3P_0)$ atoms corresponding to signal around the middle of the image (channels C1 and C6). The diamonds correspond to the experimental points. The vertical dashed lines 1 and 2 correspond to the threshold of appearance of channel C1 of 239.6 ± 1.2 nm (41740 ± 200 $cm^{-1}$), obtained from the linear fitting shown on Fig. 3(a)), and threshold of 240.99 nm (41495.6 ± 1.1 $cm^{-1}$) for the process (2) of unbound O2 photodissociation giving rise to O atoms with one of them in $^3P_0$ state. All experimental points to the right from the line 1 are attributed to channel C6.

pressure of the gas mixture (Fig. 5). The linear fitting of the experimental points in log-log scale demonstrated a third order dependence in the pressure range up to 1 bar. This result indicates that in the mentioned pressure range the dominating part of the signal originates from one-to-one clusters $C_5H_8-O_2$ since the formation of such clusters in the supersonic jet is a three-molecule collision process. Therefore, we attribute all signal of $O^+$ obtained in this work (the backing pressure was 1 bar) to the photodissociation of $C_5H_8-O_2$ one-to-one clusters.

In Fig. 6 the relative yields of channels C1 and C6 provided by the pump laser are shown. These relative yields are taken as a ratio of the sum of the integrated signals of channels C1 and C6 to the signal of channel C5. Taking this ratio allowed us to smooth the variation of the signal due to the change in the pump pulse energy and possible difference in the overlapping of the pump and probe beams in the experiments with different wavelength. The figure shows that the photoexcitation of the $C_5H_8-O_2$ complex gives rise to $O(^3P_0)$ atoms even when the exciting photon energy is less than the threshold for the photodissociation of the free $O_2$ molecule.

In Fig. 7 images of $O(^3P_0)$ atoms from two-laser experiments with $C_5H_8-O_2$ complexes are shown for different directions of polarization of the pump and probe radiation. These experiments allowed us to test the hypothesis on the nature of channel C5 suggested earlier in Ref. 1.

In Fig. 8 the integrated signal of channel C5 created by the pump laser is shown as a function of the excitation wavelength. Here the signal of channel C5 generated by the probe laser in the one-laser experiment was used for normalization. These one-laser experiments were always carried out together with corresponding two-laser experiments, so this normalization allowed us to exclude the effect of variation of probe laser energy taking place from day to day.

While all the experiments presented above have been carried out with probe laser wavelength tuned to the REMPI line of $O(^3P_0)$ atoms, all channels C1–C6 revealed have also been observed with detection of $O(^3P_J)$ atoms in the J = 2 or 1 states. The choice of presenting $O(^3P_0)$ data is due to the increase in the intensity of channel C5 with probing at the wavelength of $O(^3P_0)$ as compared with probing of $O(^3P_2)$ and $O(^3P_1)$. In this work, we have performed the most extensive two one-color experiments at similar

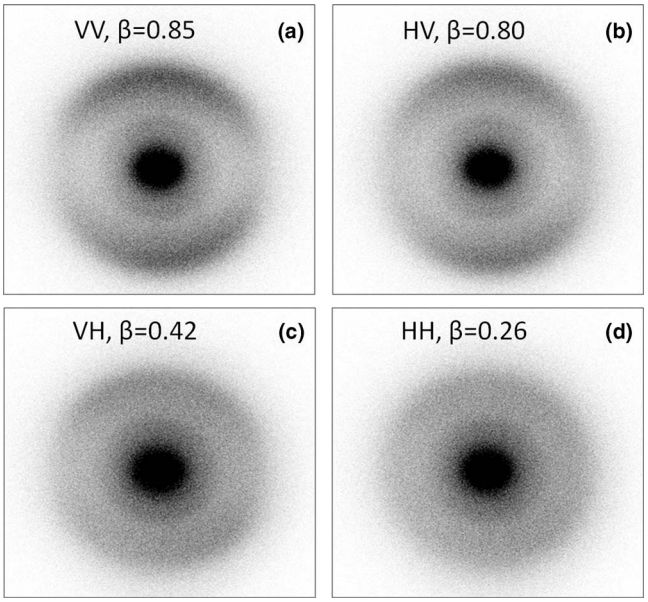


FIG. 7. Polarization dependence of $O(^3P_0)$ atoms images obtained in two-color experiments on $C_5H_8-O_2$ clusters. The wavelength of the pump laser is 240 nm, and the wavelength of the probe laser is 226.233 nm. The symbols "VV, HV, VH, and HH" indicate the directions of linear polarization of the pump and probe laser respectively. "V" corresponds the laser polarization parallel to the detector face and directed vertically with respect to the figure. "H" indicates polarization perpendicular to the detector face. The HH image is anisotropic due to the Doppler effect, which leads to slightly more efficient ionization of fragments around the middle vertical axis of the image.

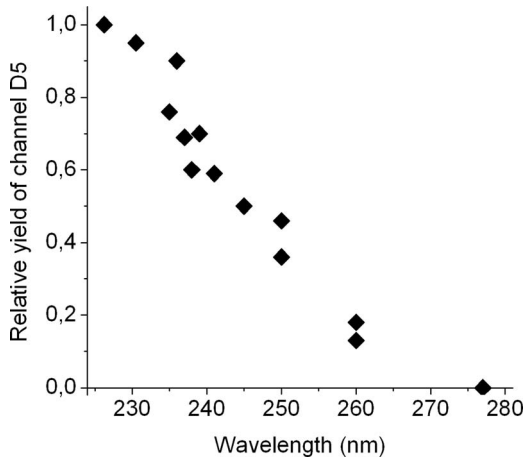


FIG. 8. Intensity of channel C5 signal as a function of the pump laser wavelength, calculated as the ratio of the integral intensity of this channel in the two-color images (after subtraction of one-color contributions) to the intensity of this channel originating from the probe laser only. According to this definition the yield of channel C5 in the one-color experiment at 226.234 nm is equal to 1.

conditions at the wavelengths of 225.564 nm and 226.234 nm corresponding to (2 + 1) REMPI of $O(^3P_2)$ and $O(^3P_0)$ states, respectively. In the first case the contribution of channel C5 to the total signal was 1.5 ± 0.6% and in the second case (this image is shown on Fig. 1(c)) it was 43 ± 1%, i.e., 30 ± 10 times higher. Similar enhancement of channel C5 at the REMPI line of $O(^3P_0)$ state was observed for other van der Waals complexes in Ref. 1. The choice of $O(^3P_0)$ allowed us to show all the channels on one image such as in Fig. 1. Similar to results for complexes studied in Ref. 1 the images for all other channels were brightest with probing of $O(^3P_2)$, less intense for $O(^3P_1)$ and lowest intensity was detected for $O(^3P_0)$. These images also differ slightly due to the small difference in excitation wavelengths corresponding to the REMPI lines of O atom in different J-states.

## IV. DISCUSSION

### A. Channel C1

Channel C1 appears as a relatively sharp ring with an energy close in value to the kinetic energy of $O(^3P_0)$ atoms produced in the one-photon dissociation of individual $O_2$ molecules,

$$O_2 + h\nu \rightarrow O(^3P_J) + O(^3P_J). \quad (2)$$

Process (2) with one product O atom in detected $^3P_0$ state and the other one in a lowest $^3P_2$ state has an appearance threshold of 41495.6 ± 1.1 $cm^{-1}$. This value is based on the $O_2$ bond energy of 41268.6 ± 1.1 $cm^{-1}$ [25] and the O atom $^3P_0$ state energy of 226.977 $cm^{-1}$.[22] The threshold for $O(^3P_0)$ atoms appearance in channel C1 can be found from the linear correlation shown in Fig. 3(a) between the measured kinetic energy of $O(^3P_0)$ atoms and energy of the exciting radiation. This threshold is equal to 41740 ± 200 $cm^{-1}$ (239.6 ± 1.1 nm) which is higher by 240 ± 200 $cm^{-1}$ compared with the dissociation of the free $O_2$. The raise in the threshold value for the photodissociation of the van der Waals complex via channel C1

$$X - O_2(^3\Sigma_g^-) + h\nu \rightarrow X - O_2(^3\Delta_u)$$
$$\rightarrow X + O(^3P_J) + O(^3P_J), \quad (3)$$

as compared with the process (2) is due to the breaking of the van der Waals bond. We suggest that channel C1 is due to excitation to the perturbed $^3\Delta_u$ Herzberg III state of $O_2$ with subsequent fast dissociation to O atoms. This mechanism was also deduced for channel C1 observed for $CH_3I-O_2$, $C_3H_6-O_2$, $C_6H_{12}-O_2$, and $Xe-O_2$ clusters in our one-color study.[1] The anisotropy parameter $\beta$ of channel C1 (Fig. 4) is positive in the entire range where it was observed, in contrast with the cases of channel C1 observed in Ref. 1, where the value of $\beta$ was observed to be more or less negative for all studied clusters. There the negative anisotropy of channel C1 was explained as a result of the T-shape (or quasi T-shape) geometry of the studied clusters where the direction from the center of X to the center of $O_2$ is (nearly) perpendicular to the O−O bond.[1,18] By analogy with the *ab initio* calculated structure of complexes $X-O_2$ with X = ethylene[14] and propylene[18] we can expect the structure of complex $C_5H_8-O_2$ to be also T- or near T-shaped. But, according to the analysis carried out in Ref. 18, even perfectly T-shaped $X-O_2$ complexes can provide angular anisotropy of the O-atom recoil directions, with variation of $\beta$ within the limits −1 to +2. In that paper it is shown that the value of $\beta$ is governed by the splitting of the total kinetic energy ($T_{tot}$) of the fragments between the translations along $X-O_2$ ($T_\parallel$) and O−O ($T_\perp$) coordinates which depends on the potential energy surface in the excited state of the complex. For the T-shaped complex the positive value of $\beta$ for O-atom angular anisotropy is expected for the sufficiently large contribution of $T_\parallel$ in $T_{tot} = T_\parallel + T_\perp$. The variation of $\beta$ value with the raise in pump quantum energy shown in Fig. 4 indicates the increase in the relative contribution of $T_\parallel$ in $T_{tot}$. The change of the $T_\parallel$ contribution is governed by the difference in the slopes of the potential energy surface of the excited state of the complex along the coordinates $X-O_2$ and O−O.

### B. Channel C2

The kinetic energy dependence of channel C2 on the photon energy (Fig. 3(b)) is linear and has a slope of 1.95 ± 0.17, which overlaps 2 within the error. This means that channel C2 is produced as in dissociation process (3) with the most of kinetic energy shared equally by two O atoms. The linear fit shown in Fig. 3(b) gives a value of the appearance threshold for this channel of 43220 ± 190 $cm^{-1}$ (231.4 ± 1.0 nm), which is 1480 ± 280 $cm^{-1}$ higher than the appearance threshold for channel C1. We attribute this difference to internal excitation ($v$) of the isoprene partner

$$X - O_2 + h\nu \rightarrow X(v) + O(^3P_J) + O(^3P_J). \quad (4)$$

The vibrational excitation can be provided by the effect of the electronic state of $O_2$ on the equilibrium geometry of the partner X molecule in complex $X-O_2$. The "vertical" excitation of $X-O_2$ giving rise to channel C1 produces $O_2$ in the $^3\Delta_u$ Herzberg III state and leaves molecule X in its ground

electronic state. We can expect, however, that the electronically excited $O_2(^3\Delta_u)$ molecule interacts with X molecule producing a change in its geometry as compared with the case of the ground state of the complex $X{-}O_2(^3\Sigma_g^-)$. The "equilibrium" geometry of X in the state $X{-}O_2(^3\Sigma_g^-)$ of the complex becomes non-equilibrium in the $X{-}O_2(^3\Delta_u)$ state. This means that the "vertical" excitation of the complex can produce the complex in the $X(v) {-}O_2(^3\Delta_u)$ excited state with partner X being vibrationally excited. This effect is similar to the change in the Franck-Condon factors for the vibronic transitions in the absorption and emission spectra for collisional $O_2{-}O_2$ pairs as compared with the spectra of unperturbed individual $O_2$ molecules, as summarized by Khan.[26] Isoprene molecule has several vibrations with wavenumbers fitting the observed shift value of 1480 ± 280 $cm^{-1}$. These wavenumbers correspond to the stretching vibrations of C=C double bonds as well as to bending vibrations of HCH groups.[27]

### C. Channel C6

The linear fit presented in Fig. 3(a) corresponds to the experimental points obtained with the wavelength of the pump laser at 239 nm and shorter. This linear fit crosses the vertical axis (where the kinetic energy is zero) at 41740 ± 200 $cm^{-1}$ (239.6 ± 1.2 nm). However, the actual signal doesn't disappear around 239.6 nm, but spans to longer wavelengths. In this region the signal appears as a small blob (Fig. 1(g)), and reliable information about the kinetic energy cannot be extracted. Instead, we plot the dependence of the intensity of the signal in the middle of the image on the pump laser wavelength (Fig. 6). The signal was still observed at $\lambda_{pump}$ = 243 nm and disappeared by $\lambda_{pump}$ = 245 nm. This means that the appearance threshold of this signal is lower than the threshold of channel C1 by at least 590 ± 200 $cm^{-1}$. We attribute the signal observed at the wavelength longer than 239.6 nm (Fig. 6) to a new channel called C6. We suppose that two mechanisms can give rise to this channel,

$$C_5H_8 - O_2 + h\nu \rightarrow C_5H_8 - O_2(^3\Delta_u) \rightarrow O(^3P_J) + C_5H_8 - O, \quad (5)$$

$$C_5H_8^* - O_2 + h\nu \rightarrow C_5H_8^* - O_2(^3\Delta_u) \rightarrow C_5H_8 + O(^3P_J) + O(^3P_J). \quad (6)$$

$X{-}O_2$ excitation below the threshold of channel C1 still provides $O_2$ molecule in the Herzberg III state $^3\Delta_u$. The final step of the process (5) can be considered as the bimolecular reaction between the electronically excited $O_2(^3\Delta_u)$ molecule and nearby molecule of isoprene giving rise to O atom plus complex $C_5H_8{-}O$. Process (5) is supposed to become possible due to the binding of O atom with isoprene. The process (6) corresponds to the borrowing of lacking energy from the complex $C_5H_8{-}O_2$ internal energy surviving due to incomplete vibrational cooling of isoprene and complex formed in the expanded jet. The processes (5) and (6) are similar to those ones supposed (see review[4]) to be responsible for the formation of ozone in oxygen by excitation of $O_2$ molecules below the dissociation limit.

### D. Channel C5

Channel C5, indicated in the images shown in Fig. 1, has kinetic energy slightly varying with wavelength within the range of 0.74 ± 0.05 eV. Since the kinetic energy of this channel was basically independent of the wavelength of the pump laser, we suspect that the probe laser (with fixed wavelength) was responsible not only for the ionization of $O(^3P_0)$ atoms but also for the formation of $O(^3P_0)$ atoms with this kinetic energy.

In the paper[1] the precursor of O atoms from channel C5 was suggested to be the superoxide anion $O_2^-$ because its photodissociation via a one-photon allowed transition at the wavelength used could provide the O-atoms with observed energy. To test this hypothesis we have carried out the experiments directed to the detection of the superoxide anion. First, consider the results of the polarization experiments presented in Fig. 7. In this figure there are images obtained with different polarizations of the pump and probe radiation. In these experiments, the photodissociation of $C_5H_8{-}O_2$ is mainly provided by pump laser radiation at 240 nm. This conclusion is deduced from the depletion by the pump radiation of C1 channel provided by the probe laser itself. The depletion factor was measured to be about 75%. The precursor of channel C5 should thus appear mainly due to the pump pulse. Photodissociation of this precursor giving rise to $O(^3P_0)$ atoms of C5 channel, however, is provided mainly by the probe pulse at about 226 nm, as was deduced above from the independence of the kinetic energy of the O atoms of channel C5. This is also indicated by the drop in the angular anisotropy of channel C5 from 0.85 to 0.42 when the polarization of the probe laser is changed from vertical (VV) to horizontal (VH). At the same time, changing the pump laser polarization from V to H provides only a slight reduction by 0.05 of $\beta$ for the channel C5 anisotropy (VV and HV experiments) which is within the experimental uncertainty. This domination of probe radiation in the photodissociation of the C5 channel precursor indicates probably the higher absorption cross section at 226 nm as compared with 240 nm for the precursor. The results of our experiments allow us to conclude that the precursor of C5 channel is produced by the pump laser and is then photodissociated by the pulse of probe laser.

In the absence of a probe pulse the supposed $O_2^-$ precursor could be detected. To detect this anion we have changed the polarity of electrodes of the imaging setup. The quantity of these precursors should not be less than the quantity of $O^+$ ions in channel C5 produced by the probe radiation. This last quantity corresponds to about 75% of the C5 image in Fig. 7. That should be easily detected if it is ionic like $O_2^-$. We observe, however, no $O_2^-$ or any other negative ions. This unambiguously eliminates $O_2^-$ as a source of the O atoms of channel C5.

In Ref. 1, the precursor of C5 channel was concluded to contain only oxygen because the kinetic energy and angular anisotropy of the O atoms from channel C5 did not depend

on the type of the partner molecule X in the complex X−$O_2$. Above, we excluded the superoxide anion $O_2^-$ as a precursor. Another ion, $O_2^+$, can be also excluded because photoexcitation of this ion should provide not only an O atom probed resonantly by REMPI but also an $O^+$ ion which should provide a contribution to the image at the wavelengths out of REMPI lines of O atoms as well. According to the data described in Ref. 1, the imaged ions were observed only when the laser was resonant with the REMPI lines of $O(^3P_J)$ atoms. We can thus conclude that neutral oxygen in some electronic state of $O_2$ is the precursor of O atoms from channel C5 in our experiments on the X−$O_2$ complexes carried out in Ref. 1 and in the current paper. Kinetic energy analysis shows that only the first excited singlet state $O_2(^1\Delta_g)$ can be the precursor of channel C5. The photodissociation of singlet oxygen by the probe laser in the region of REMPI lines of $O(^3P_J)$ provides oxygen atoms mainly in $^3P_0$ state as it is revealed in the current paper (see Results). The predominance of $O(^3P_0)$ over $O(^3P_2)$ and $O(^3P_1)$ was also observed for channel C5 in complexes X−$O_2$ studied in Ref. 1. At the wavelength 226.233 nm used in the current work the photodissociation of singlet oxygen thus proceeds mainly via the equation

$$O_2(^1\Delta_g) + h\nu(5.48\,\text{eV}) \rightarrow O(^3P_0) + O(^3P_J) \qquad (7)$$

providing O atoms with total kinetic energy release equal to 1.28 eV. This number is calculated using the value of the bond energy for the $O_2$ ground state of $D_0 = 41268.6 \pm 1.1$ cm$^{-1}$,[25] the value of the energy gap of 7882.39 cm$^{-1}$ between $v = 0$ levels of the ground state and $a\,^1\Delta_g$ state of $O_2$,[28] and the $J = 0$ level O atom energy value from.[22] The kinetic energy of the detected $O(^3P_0)$ atoms arising from channel C5 must be $E_t = 0.64$ eV. The energy match with measured value $E_t = 0.74 \pm 0.05$ eV is not perfect, but this is the best match among all low-lying and long-lifetime states of $O_2$.

The broad shape of the C5 ring means that the precursor of O atoms has a spread in kinetic energy and/or has a distribution over the rovibrational levels. Both of those effects must make the average radius of the ring larger. The vibrational quantum of $a\,^1\Delta_g$ state equals 1483.5 cm$^{-1}$ (0.18 eV).[28] This means that the excitation with one vibrational quantum leads to a perfect match between the calculated kinetic energy release in process (7) and the kinetic energy measured. Channel C5 was observed in Ref. 1 for complexes of methyl iodide $CH_3I$−$O_2$ and propylene $C_3H_6$−$O_2$ with the kinetic energy of $O(^3P_2)$ atom products $E_t = 0.69 \pm 0.04$ eV, measured at 225.65 nm. The expected value for process (7) with $h\nu = 5.49$ eV and $O(^3P_J) = O(^3P_2)$ and vibrationally unexcited singlet oxygen as a precursor is equal to the value of 0.66 eV which fits the measured value very well. Thus, for all three complexes where channel C5 was observed, we can deduce the formation of singlet oxygen $O_2(^1\Delta_g)$ with no or small vibrational excitation.

The atoms $O(^3P_0)$ of channel C5 are produced in the photodissociation of singlet oxygen $O_2(^1\Delta_g)$ mainly by the probe radiation. Starting from this state probing radiation with quantum energy of 5.48 eV can populate in a one-photon transition the Herzberg states ($A\,^3\Sigma_u^+$, $c\,^1\Sigma_u^-$, $A'\,^3\Delta_u$) or the $B\,^3\Sigma_u^-$ Schumann-Runge state of oxygen. All of these optical transitions are forbidden, therefore one can expect the dissociation of $O_2(a\,^1\Delta_g)$ to have a low cross-section. This is in agreement with our results where we observed an increase in the relative contribution of channel C5 to other channels with increasing power of the probe laser. The rise of the contribution was observed over the entire range of achievable photon fluxes up to $10^{21}$ photons/cm$^2$, indicating that the absorption cross section was at least not higher than $10^{-21}$ cm$^2$. It also means that our pump laser was never able to dissociate all $O_2(a\,^1\Delta_g)$ produced by the pump laser. Therefore, we can make the conclusion that the actual production of $O_2(a\,^1\Delta_g)$ is quite high and its photodissociation provides more than 50% of the total production of $O(^3P_0)$ in our experiments for the $C_5H_8$−$O_2$ complex. This indicates high yield of singlet oxygen in the photoexcitation of complex $C_5H_8$−$O_2$ in this spectral region.

As a mechanism of singlet oxygen photo-generation we suggest a cooperative transition in the complex with simultaneous change of the spin of both partners

$$^1X - {}^3O_2 + h\nu \rightarrow {}^3X - O_2(a\,^1\Delta_g) \rightarrow {}^3X + O_2(a\,^1\Delta_g), \qquad (8)$$

with oxygen being excited to the singlet *a* state and partner X being excited to the triplet $^3X$ state. These cooperative transitions were suggested by Dijkgraaf and Hoijtink to be responsible for the oxygen-induced transitions in aromatics located in the spectrum to the blue relative to the oxygen-induced singlet-triplet transitions in X molecule.[29] Later, Minaev *et al.* calculated *ab initio* the oscillator strength for several types of the cooperative transitions in the complexes $C_2H_4$−$O_2$ (Ref. 30) and $C_6H_6$−$O_2$.[31] They found strong oscillator strength for the transitions of the type (8) at a X–$O_2$ pair distance of 3–4 Å which covers the values of distance in van der Waals complexes of oxygen, as calculated in Ref. 18. Our experimental results indicating only a small amount of vibrational excitation of singlet oxygen indicate the cooperative transition (8) as a source of $O_2(a\,^1\Delta_g)$. The probability of vibrational excitation of $O_2(a\,^1\Delta_g)$ arising in process (8) is governed by the Franck-Condon factor values. In the X–$O_2$ van der Waals complex the influence of X on the shape of the potential curve of $O_2$ in the ground $^3\Sigma_g^-$ and excited $^1\Delta_g$ states should not be essential due to the long X–$O_2$ distance. For estimation we can thus use the Franck-Condon values for the individual $O_2$ molecule. According to the calculated data presented in Ref. 32, the maximum value of the Franck-Condon factor for transitions starting from the ground vibronic state belongs to the transition ($^3\Sigma_g^-$, $v' = 0$) ← ($^3\Sigma_g^-$, $v'' = 0$) and is equal to about 0.99. This means that cooperative transition (8) should provide vibrationally non-excited $O_2(a\,^1\Delta_g)$. If we consider the influence of the neighbor triplet molecule $X(T_1)$ on the shape of the potential curve of $O_2$ in the excited $^1\Delta_g$ state, then some probably small vibrational excitation of $O_2(a\,^1\Delta_g)$ could be expected. This influence is similar to that described in the Discussion devoted to the C2 channel. We can thus consider the absence of a substantial vibrational excitation in $O_2(a\,^1\Delta_g)$ detected as indication of the cooperative transition (8) in the X–$O_2$ van der Waals complex as a source of singlet oxygen.

Process (8) becomes possible if the energy of the photon absorbed ($h\nu \approx 5.5$. eV) is sufficient for simultaneous

("vertical" or near that) excitation of oxygen in the singlet ($a\,^1\Delta_g$) state and X molecule in the triplet state. For the X–$O_2$ complexes (X=$CH_3I$, $C_3H_6$, $C_5H_8$), where $O_2(a\,^1\Delta_g)$ has been detected, this condition is fulfilled. The "vertical" excitation of $CH_3I$ into the triplet $^3Q_1$ state takes 4.1 eV, as experimentally determined by Gedanken and Rowe.[33] The "vertical" excitation of $C_3H_6$ is expected to be close to that for $C_2H_4$ which is calculated to be of 4.5 eV.[34] For isoprene $C_5H_8$ we can estimate this "vertical" gap to be close to that for butadiene which is calculated to be of 3.2 eV.[34] Together with the energy of 0.977 eV [28] for transition of oxygen to the ground vibrational state of a $^1\Delta_g$ term these values provide as a sum ≈5.1, 5.5, and 4.2 eV, respectively, which are close to or less than the exciting quantum energy 5.5 eV. For isoprene the cooperative process (8) with excitation of the second triplet state $T_2$ of $C_5H_8$ can be responsible for the formation of $O_2(a\,^1\Delta_g)$ in our experiments. The "vertical" energy of $T_2$ state excitation can be estimated to be close to that for butadiene which was calculated to be equal to 5.1 eV.[34] The "vertical" energy of cooperative transition is estimated to be of 6.1 eV. So the spectral range of our pump laser tuning 213–277 nm ($h\nu$ = 5.8–4.5 eV) corresponds to the red wing of the absorption band. In this case the cross section for cooperative absorption and so the yield of $O_2(a\,^1\Delta_g)$ should decrease with moving the wavelength of pump laser to the red that fits our experimental data shown on Fig. 8.

### E. Channel C4

Channel C4 was observed at the excitation wavelengths 222 and 213 nm (see Fig. 1). We believe that our channel C4 is similar to that for channel C4 in the one-color study[1] for $CH_3I$–$O_2$ clusters. There, this channel was concluded to be due to photodissociation of molecular oxygen in the second singlet state

$$O_2(b\,^1\Sigma_g^+) + h\nu \rightarrow O(^3P_J) + O(^1D).$$

By analogy with the formation of $O_2(a\,^1\Delta_g)$ we suggest the cooperative excitation of the complex as a source of $O_2(b\,^1\Sigma_g^+)$

$$X(S_0) - O_2(^3\Sigma_g^-) + h\nu \rightarrow X(T_1) - O_2(b\,^1\Sigma_g^+) \rightarrow X(T_1) + O_2(b\,^1\Sigma_g^+), \quad (9)$$

which is similar to process (8). 1.63 eV [28] is necessary for a transition of oxygen to the ground vibrational state of the $b\,^1\Sigma_g^+$ state. For $C_5H_8$–$O_2$ the "vertical" energy to provide transition (9) is equal to about 4.8 eV, which is less than excitation energy of 5.5 eV. For $CH_3I$–$O_2$ the "vertical" energy for transition (9) is equal to about 5.7 eV which is close to 5.5 eV as well.

At the same time we can not exclude the contribution to this channel of the process (4) with vibrational excitation of isoprene by about two times higher than in channel C2.

## V. CONCLUSION

Two-laser experiments have been carried out to investigate the photophysics and photochemistry of $C_5H_8$–$O_2$, the van der Waals complex of isoprene with oxygen, which is a model for corresponding collisional complexes in the atmosphere. The presence of a neighbor isoprene molecule in the $C_5H_8$–$O_2$ van der Waals complex was found to dramatically affect the photophysics and photochemistry of oxygen. Velocity map imaging of O atoms resulting from UV-photoexcitation of $C_5H_8$–$O_2$ in the wavelength range of 213–277 nm allowed us to distinguish up to 5 channels differing in product oxygen atom kinetic energy and angular anisotropy recoil directions, indicating supramolecular UV-photophysics and photochemistry of $C_5H_8$–$O_2$. These results, together with data for other X–$O_2$ complexes studied in our one-laser experiments,[1] have been used for the assignment of the transitions and dissociation mechanisms observed.

Three channels are deduced to be due to one-photon excitation into the Herzberg III state of $O_2$ perturbed by the isoprene molecule. This excitation results in the dissociation $C_5H_8$–$O_2$ + $h\nu$ → $C_5H_8(v)$ + O + O when the energy of exciting quantum is higher than the photodissociation threshold, estimated to be of about 41740 ± 200 $cm^{-1}$. Two observed kinetic energy modes of O atom were interpreted to be due to this dissociation with formation of unexcited isoprene molecule (channel C1 in the notation used in the text) and rovibrationally excited $C_5H_8(v)$ with an internal energy of 1480 ± 280 $cm^{-1}$ (channel C2). The variation of angular anisotropy of these channels through the excitation spectrum has been interpreted as being due to a change in the characteristics of the potential energy surface, different parts of which are populated at different wavelengths. A third channel (C6) was observed even when the exciting quantum energy was less than the photodissociation threshold by 590 ± 200 $cm^{-1}$. This channel was attributed to the excitation of Herzberg III state of $O_2$ in complex followed by bimolecular reaction in the complex with the scheme $C_5H_8 - O_2 + h\nu \rightarrow C_5H_8 - O_2(^3\Delta_u) \rightarrow O + C_5H_8 - O$ and/or by borrowing the lacking energy from the incompletely cooled intracomplex $C_5H_8^* - O_2$ vibrational degrees of freedom with the scheme $C_5H_8^* - O_2 + h\nu \rightarrow C_5H_8^* - O_2(^3\Delta_u) \rightarrow C_5H_8 + O(^3P_J) + O(^3P_J)$.

Two other observed channels (C5 and C4) correspond to O atoms produced by photodissociation of the excited singlet states $a\,^1\Delta_g$ and $b\,^1\Sigma_g^+$ of oxygen as precursors. This indicates the formation of singlet oxygen $O_2(a\,^1\Delta_g)$ and $O_2(b\,^1\Sigma_g^+)$ after excitation of the $C_5H_8$–$O_2$ complex. Excitation to the CT state as a source of channel C5, which was suggested in,[1] was eliminated on the basis of the results obtained. A cooperative excitation of the complex with simultaneous change of the spin of both partners $^1X$–$^3O_2$ + $h\nu$ → $^3X$–$^1O_2$ → $^3X$ + $^1O_2$ is suggested as the source of singlet oxygen $O_2(a\,^1\Delta_g)$ and $O_2(b\,^1\Sigma_g^+)$. This cooperative excitation is in agreement with the small or no vibrational excitation of $O_2(a\,^1\Delta_g)$ deduced from kinetic energy of O atoms produced in channel C5 from complex $C_5H_8$-$O_2$ in the current paper as well as from $C_3H_6$–$O_2$ and $CH_3I$–$O_2$ in Ref. 1. The formation of $O_2(a\,^1\Delta_g)$ from $C_5H_8$–$O_2$ was observed at $\lambda_{pump}$ = 213–260 nm with the yield going down towards the long wavelength edge of this interval. This spectral profile is interpreted as the red-side wing of the band of cooperative

transition $^1X–^3O_2 + h\nu \rightarrow {}^3X(T_2) - {}^1O_2(a\,{}^1\Delta_g)$ in complex $C_5H_8–O_2$.

## ACKNOWLEDGMENTS

We gratefully acknowledge financial support from the Netherlands Organization for Scientific Research (NWO) under the programs Molecular Atmospheric Physics (MAP-09), NWO-CW ECHO project number 700.55.025, and NWO Russia-Netherlands Cooperative Research Grant 047.009.001 as well as the financial support of this work by Russian Foundation for Basic Research (Grant No. 09-03-00310-a). The authors also thank Professor W. van der Zande for the use of his MOPO-laser.

[1] A. V. Baklanov, G. A. Bogdanchikov, K. V. Vidma, D. A. Chestakov, and D. H. Parker, J. Chem. Phys. **126**, 124316 (2007).
[2] D. H. Parker, Acc. Chem. Res. **33**, 563 (2000).
[3] A. J. Blake and D. G. McCoy, J. Quant. Spectrosc. Radiat. Transf **38**, 113 (1987).
[4] S. Koda and K. Sugimoto, J. Photochem. Photobiol. C **4**, 215 (2003).
[5] D. F. Evans, J. Chem. Soc. **1953**, 345.
[6] J. Goodman and L. E. Brus, J. Chem. Phys. **67**, 1482 (1977).
[7] V. R. Blok, O. L. Lebedev, and N. G. Mekhryakova, Dokl. Akad. Nauk SSSR **249**, 633 (1979).
[8] Y. Oshima, Y. Okamoto, and S. Koda, J. Phys. Chem. **99**, 11830 (1995).
[9] G. Y. Zelikina, V. V. Bertsev, A. P. Burtsev, and M. B. Kiseleva, Opt. Spectrosc. **81**, 685 (1996); G. Y. Zelikina, M. B. Kiseleva, A. P. Burtsev, and V. V. Bertsev, *ibid.* **85**, 520 (1998).
[10] B. Coquart and D. A. Ramsay, Can. J. Phys. **64**, 726 (1986).
[11] S. Koda and H. Kajihara, Bull. Chem. Soc. Jpn. **70**, 1225 (1997).
[12] P. Bernath, M. Carleer, S. Fally, A. Jenouvrier, A. C. Vandaele, C. Hermans, M. F. Merienne, and R. Colin, Chem. Phys. Lett. **297**, 293 (1998).
[13] G. DeBoer and M. A. Young, J. Chem. Phys. **106**, 5468 (1997).
[14] G. DeBoer, A. P. Prince, and M. A. Young, J. Chem. Phys. **115**, 3112 (2001).
[15] A. Giardini Guidoni, A. Paladini, M. Veneziani, R. Naaman, and T. M. Di Palma, Appl. Surf. Sci. **154–155**, 186 (2000).
[16] B. F. Parsons and D. W. Chandler, J. Phys. Chem. A **107**, 10544 (2003).
[17] D. Chestakov, S.-M. Wu, G. Wu, D. H. Parker, A. T. J. B. Eppink, and T. N. Kitsopoulos, J. Phys. Chem. A **108**, 8100 (2004).
[18] K. V. Vidma, G. A. Bogdanchikov, A. V. Baklanov, D. A. Chestakov, and D. H. Parker, J. Chem. Phys. **133**, 194306 (2010).
[19] J. H. Seinfeld and S. N. Pandis, *Atmospheric Chemistry and Physics: From Air Pollution to Climate Change* (Wiley, 1998), p. 1326.
[20] A. T. J. B. Eppink and D. H. Parker, Rev. Sci. Instrum. **68**, 3477 (1997).
[21] E. Wrede, S. Laubach, S. Schulenburg, A. Brown, E. R. Wouters, A. J. Orr-Ewing, and M. N. R. Ashfold, J. Chem. Phys. **114**, 2629 (2001).
[22] Yu. Ralchenko, A. E. Kramida, J. Reader, and NIST ASD Team, *NIST Atomic Spectra Database*, version 3.1.5 (National Institute of Standards and Technology, Gaithersburg, MD, 2008), see http://physics.nist.gov/asC3.
[23] V. Dribinski, A. Ossadtchi, V. A. Mandelshtam, and H. Reisler, Rev. Sci. Instrum. **73**, 2634 (2002).
[24] R. N. Zare, Mol. Photochem. **4**, 1 (1972).
[25] P. C. Cosby and D. L. Huestis, J. Chem. Phys. **97**, 6108 (1992).
[26] A. U. Khan, in *Singlet $O_2$*, edited by A. A. Frimer (CRC, Boca Raton, 1985), Vol. 1, pp. 39–79.
[27] L. M. Sverdlov, M. A. Kovner, and E. P. Krainov, *Vibrational Spectra of Polyatomic Molecules* (Wiley, 1973), p. 644.
[28] K. P. Huber and G. Herzberg, "Constants of Diatomic Molecules" (data prepared by J. W. Gallagher and R. D. Johnson III) in NIST Chemistry WebBook, NIST Standard Reference Database Number 69, edited by P. J. Linstrom and W. G. Mallard, National Institute of Standards and Technology, Gaithersburg, MD 20899, http://webbook.nist.gov (retrieved July 20, 2012).
[29] C. Dijkgraaf and G. J. Hoijtink, Tetrahedron **19**(Suppl. 2), 179 (1963).
[30] B. F. Minaev, V. V. Kukueva, and H. Ågren, J. Chem. Soc., Faraday Trans. **90**, 1479 (1994).
[31] B. F. Minaev, K. V. Mikkelsen, and H. Ågren, Chem. Phys. **220**, 79 (1997).
[32] R. W. Nicholls, J. Res. Natl. Bur. Stand., Sect. A **69A**, 369 (1965).
[33] A. Gedanken and M. D. Rowe, Chem. Phys. Lett. **34**, 39 (1975).
[34] M. Schreiber, M. R Silva-Junior, S. P. A. Sauer, and W. Thiel, J. Chem. Phys. **128**, 134110 (2008).